Polymer Chemistry

ROYAL SOCIETY OF CHEMISTRY

PAPER

View Article Online
View Journal | View Issue

Cite this: *Polym. Chem.*, 2023, **14**, 1727

One-pot catalyst-switching synthesis of thermoresponsive amphiphilic diblock copolymers consisting of poly(*N*,*N*-diethylacrylamide) and biodegradable polyesters†

Xiangming Fu, [a] Yanqiu Wang,[a] Liang Xu,[a] Atsushi Narumi, [b] Shin-ichiro Sato, [c] Xiande Shen*[a,d] and Toyoji Kakuchi *[a,c,d]

Received 22nd February 2023,
Accepted 17th March 2023

DOI: 10.1039/d3py00195d

rsc.li/polymers

A method for the syntheses of thermoresponsive amphiphilic diblock copolymers through sequential organocatalyzed polymerizations of vinyl-based and lactone-based monomers using group transfer polymerization (GTP) and ring-opening polymerization (ROP), respectively, is described. The organocatalysts were switched between the two polymerization stages and all syntheses could be conducted in a one-pot manner. The polymerization systems directly produced diblock copolymers composed of poly(*N*,*N*-diethylacrylamide) and biodegradable polyesters (poly(ε-caprolactone), poly(trimethylene carbonate), and poly(L-lactide) in various content ratios. Aqueous solutions of the obtained block copolymers below their cloud point temperatures (T_{cp}) were carefully characterized, revealing a close relationship among the structures of the block copolymers, T_{cp}, and micellar forming properties below the T_{cp}.

Introduction

Amphiphilic copolymers modified with hydrophobic groups self-assemble in water to form nano aggregates, such as micelles and vesicles that have three-dimensional structures, such as spheres and rods.[1–4] The morphology of these aggregates is highly dependent on the molecular design of the amphiphilic copolymer and is determined by the primary polymer structure, including the structural properties and balance of hydrophilic and hydrophobic moieties, composition, chain length, and chain configuration.[5,6] Amphiphilic copolymers with different linkage structures between hydrophilic and hydrophobic moieties are designated as block copolymers with hydrophilic and hydrophobic chains linked in series, graft copolymers with hydrophilic main chains and hydrophobic side chains, or random and alternating copolymers of hydrophilic and hydrophobic side chains.[7–10] The development of precision polymerization techniques, controlled/living radical polymerization (CLRP) as a representative example, has enabled facile syntheses of a variety of block copolymers.[11–13] For example, many amphiphilic block copolymers with poly(*N*-isopropylacrylamide) (PNIPAm) as a thermoresponsive segment have been designed and synthesized using appropriate CLRPs, such as nitroxide mediated polymerization, metal catalyzed atom transfer radical polymerization, and reversible addition–fragmentation chain transfer polymerization.[14–19] Poly(*N*,*N*-disubstituted acrylamide)s are thermoresponsive, and poly(*N*,*N*-diethylacrylamide) (PDEAm) is commonly used in the synthesis of various thermoresponsive architectures, including block copolymers, graft copolymers, cyclic polymers, and star-shaped polymers using CLRP or controlled/living anionic polymerization.[20–24] We have reported that the organocatalytic group transfer polymerization (GTP) of acrylamide monomers using silyl ketene acetal (SKA) and silyl ketene aminal (SKAm) is a reliable synthetic method for obtaining well-defined polyacrylamides. Furthermore, we developed a new GTP method without relying on SKA and SKAm initiating agents, *i.e.*, the hydrosilylation-promoted GTP of acrylamide monomers using a Lewis acid of $B(C_6F_5)_3$ and a hydrosilane (R_3SiH).[25] Additionally, an α-end functionalized polyacrylamide was synthesized by the hydrosilylation-promoted GTP of acrylamide monomers using

[a]*Research Center for Polymer Materials, Engineering Research Center of Optoelectronic Functional Materials, Ministry of Education, School of Materials Science and Engineering, Changchun University of Science and Technology, Weixing Road 7989, Jilin 130022, China. E-mail: kakuchi@eng.hokudai.ac.jp; Fax: +81-11-706-6602; Tel: +81-11-706-6602*
[b]*Graduate School of Organic Materials Science, Yamagata University, 4-3-16 Jonan, Yonezawa, Yamagata 992-8510, Japan*
[c]*Division of Applied Chemistry, Faculty of Engineering, Faculty of Engineering, Hokkaido University, Sapporo, Hokkaido 060-8628, Japan*
[d]*Chongqing Research Institute, Changchun University of Science and Technology, No. 618 Liangjiang Avenue, Longxing Town, Yubei District, Chongqing City 401135, China*

† Electronic supplementary information (ESI) available. See DOI: https://doi.org/10.1039/d3py00195d

$B(C_6F_5)_3$ and functionalized methacrylamide as a latent initiator.[26]

Since Hedrick *et al.* reported the living ring-opening polymerization (ROP) of lactide to a well-defined polylactide using 4-dimethylaminopyridine as an organocatalyst, many developments have been reported for the organocatalytic ROP reaction in terms of applicable monomers, organocatalyst types, and controlled/living systems.[27] Cyclic ethers, such as ethylene oxide (EO) and glycidyl ether, cyclic esters, such as δ-valerolactone (δ-VL), ε-caprolactone (ε-CL), and L-lactide (L-LA), and cyclic carbonates rare commonly studied biocompatible and biodegradable monomers for ROP.[28–32] There are many types of organocatalysts, including imidazoles, amines, amidines ammonium salts, phosphonium and phosphazene bases, and N-heterocyclic carbenes.[33–36] We reported that diphenyl phosphate (DPP) is an effective organocatalyst for controlled/living ROP of δ-VL, ε-CL, and trimethylene carbonate (TMC), but is a poor catalyst for ROP of L-LA.[37–39] Hadjichristidis *et al.* used phosphazene base *t*-Bu-P_2 to improve the applicable monomer limitations and successfully produced copolymers with various block combinations by the *t*-Bu-P_2-catalyzed ROPs of EO, δ-VL, ε-CL, TMC, and L-LA.[40–44]

Here we report the "one-pot catalyst-switching" method for synthesizing amphiphilic diblock copolymers without separating the first block segment using two different controlled/living addition polymerization methods, GTP and ROP, by switching to the appropriate organocatalyst for each polymerization (Scheme 1).[45–50] The one-pot synthetic pathway is described as follows: (1) equimolar amounts of MAm-OTBDMS and Me_2EtSiH using $B(C_6F_5)_3$ for 1,6-hydrosilylation yields the $SKAm^{Me2Et}$-OTBDMS initiator. (2) Me_3SiNTf_2-catalyzed GTP of DEAm using $SKAm^{Me2Et}$-OTBDMS yields PDEAm-OTBDMS. (3) Deprotection of PDEAm-OTBDMS using tetra-*n*-butylammonium fluoride (TBAF) in the polymerization system yields macroinitiator PDEAm-OH. (4) Lastly, switching the catalyst from Me_3SiNTf_2 to *t*-Bu-P_2 enables the ROPs of cyclic esters initiated by PDEAm-OH to synthesize PDEAm-*block*-polyesters (PDEAm-*b*-PEs). Thermoresponsive behaviors of the resulting PDEAm-*b*-PEs were evaluated by measuring the cloud-point temperature (T_{cp}) and the aggregation properties below and above the T_{cp} are discussed in terms of changes in the hydrodynamic radius (R_h).

Experimental

Materials

N-(2-*tert*-Butyldimethylsiloxyethyl)-*N*-methylmethacrylamide (MAm-OTBDMS) was prepared according to the previously reported method.[26] Dry tetrahydrofuran (99.5%) and dimethylethylsilane (Me_2EtSiH; 99.5%) were purchased from Kanto Chemical, Co., Inc. (Tokyo, Japan). *N*,*N*-Diethylacrylamide (DEAm) was purchased from Tokyo Chemical Industry Co., Ltd (TCI; Tokyo, Japan) and used after distillation over CaH_2 under reduced pressure. Tris(pentafluorophenyl)borane ($B(C_6F_5)_3$) was purchased from TCI and was used after purification by recrystallization from *n*-hexane at −30 °C. 1-*tert*-Butyl-2,2,4,4,4pentakis(dimethylamino)-2λ^5,4λ^5-catenadi(phosphazene) (*t*-Bu-P_2) was purchased from Sigma-Aldrich (St Louis, MO, USA). Extra dry dichloromethane (>99.5%; water content, <50 ppm) delivered over molecular sieves was purchased from Energy Chemicals Co., Inc. (Anhui, China). All other reagents were used as received without further purification.

Measurements

^{1}H NMR spectra were recorded by Bruker Avance III HD 500. Polymerization solutions were prepared in a Mikrouna glove box equipped with a gas purification system (molecular sieves and copper catalyst) and a dry argon atmosphere (H_2O, O_2, <1 ppm). Moisture and oxygen contents in the glove box were monitored by sensors MK-XTR-100 and MK-OXSEN-1, respectively. Number-average molecular weights ($M_{n,SEC}$) and size distribution ($Đ$) of the polymers were measured by size exclusion chromatography (SEC) at 60 °C using an Agilent high perform-

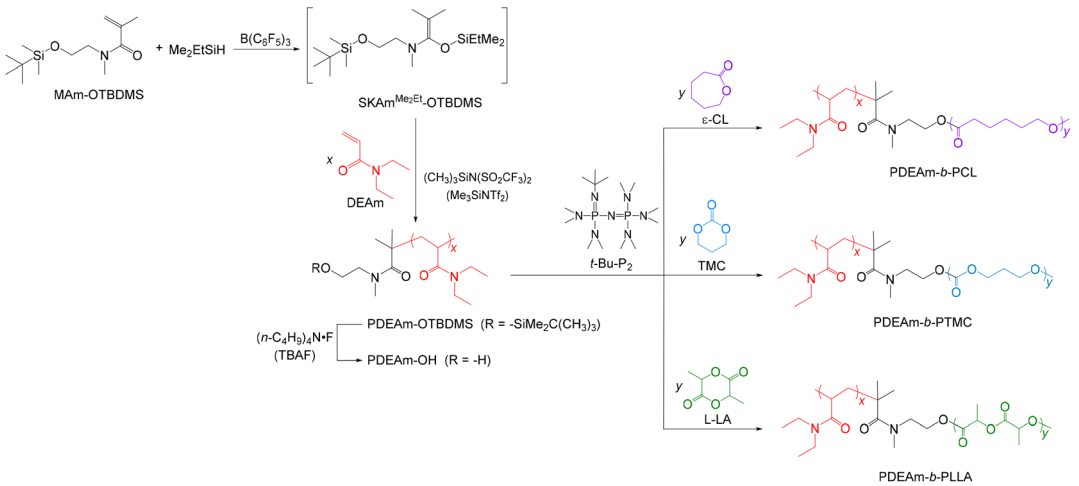

Scheme 1 One-pot catalyst-switch syntheses of PDEAm-*b*-PEs by the controlled/living GTP and ROP using $B(C_6F_5)_3$ and *t*-Bu-P_2, respectively.

ance liquid chromatography system (1260 Infinity II) in *N*,*N*-dimethylformamide (DMF) containing lithium chloride (0.01 mol L^{-1}) at the flow rate of 1.0 mL min^{-1} using Agilent Polar Gel-M (exclusion limit, 2×10^4 g mol^{-1}) and Polar Gel-M (exclusion limit, 4×10^6 g mol^{-1}) columns (7.5 × 300 mm; average bead size, 5 μm). Cloud-point measurements were performed on ultraviolet–visible (UV-vis) spectrophotometer (Jasco V-770, Tokyo, Japan) equipped with a Jasco CTU-100 temperature-controller. The path length was 10 mm and temperature was increased at a rate of 1 °C min^{-1}. Changes in transmittance with temperature were recorded u at a wavelength of 500 nm. Hydrodynamic radius (R_h) of the obtained polymers was analyzed using a Dyna Pro Nanostar® (Wyatt Technology, Sant Barbara, Ca, USA).

One-pot synthesis of PDEAm-*b*-PEs with catalyst-switching

A typical procedure for the synthesis of PDEAm-*b*-PCL is described as follows: in a glove box under an argon atmosphere, $B(C_6F_5)_3$ (25.5 mg, 50.0 μmol) was added to a solution of MAm-OTBDMS (56.5 mg, 0.22 mmol) and Me_2EtSiH (26.4 μL, 0.20 mmol) in 0.95 mL of CH_2Cl_2 in a round-bottom flask at room temperature. After stirring the reaction solution for 12 h, an aliquot was removed from the reaction mixture and the quantitative formation of SKAmMe_2Et-OTBDMS was confirmed by ^{1}H NMR. DEAm (1.27 g, 10.0 mmol) and CH_2Cl_2 (4.75 mL) were added to the round bottom flask, and then 0.1 mL of Me_3SiNTf_2 in CH_2Cl_2 (10.0 μmol, 0.1 mol L^{-1}) was added to catalyze GTP. After 30 min, PDEAm$_{50}$-OTBDMS was obtained. Quantitative consumption of DEAm was confirmed using ^{1}H NMR measurements of aliquots taken from the polymerization mixture. To deprotect PDEAm$_{50}$-OTBDMS, 3.0 mL of tetrabutylammonium fluoride (TBAF) in THF (3.0 mmol, 1.0 mol L^{-1}) was added to the round-bottom flask, and the entire mixture was stirred for 36 h. This solution became the stock solution of PDEAm$_{50}$-OH (0.20 mol) with an $M_{n,SEC}$ of 6.2 kg mol^{-1} and a $Đ$ of 1.08. In a separate test tube, PDEAm-OH stock solution (2.0 mL, 40 mmol) was mixed with a solution of ε-CL (228.2 mg, 2.0 mmol) in toluene (0.2 mL), and then *t*-Bu-P_2 (36.8 mg) was added to catalyze ROP. After 12 h, the crude polymer was purified by precipitation with cold hexane to afford PDEAm$_{50}$-*b*-PCL$_{50}$ as a white solid with an $M_{n,SEC}$ of 12.3 kg mol^{-1} and a $Đ$ of 1.10. Similarly, ROP of trimethylene carbonate (TMC, 204.2 mg, 2.0 mmol) using a stock solution of PDEAm-OH (2.0 mL, 40 mmol) yielded PDEAm$_{50}$-*b*PTMC$_{50}$ with a $M_{n,SEC}$ of 11.2 kg mol^{-1} and a $Đ$ of 1.17 and also L-lactide (L-LA, 288.2 mg, 2.0 mmol) yielded PDEAm$_{50}$-*b*-PLLA$_{50}$ with an $M_{n,SEC}$ of 12.5 kg mol^{-1} and $Đ$ of 1.17.

Results and discussion

Formation of functional SKAm initiator

Scheme 1 shows the one-pot synthesis of PDEAm-*b*-PEs using two controlled/living polymerizations, GTP and subsequent ROP, using the appropriate organocatalysts for each polymerization stage. To prepare the SKAm initiator, a small excess of latent initiator should be used to avoid the presence of free hydrosilane in the reaction mixture. We applied the $B(C_6F_5)_3$-catalyzed hydrosilylation of MAm-OTBDMS with Me_2EtSiH ($[MAm\text{-}OTBDMS]_0/[Me_2EtSiH]_0/[B(C_6F_5)_3]_0$ = 1.1/1.0/0.25) in CH_2Cl_2 to yield a SKAm initiator possessing a *tert*-butyldimethylsilyl (TBDMS)-protected hydroxyl group (SKAm^{Me2Et}-OTBDMS). The formation of SKAm was confirmed by ^{1}H NMR spectroscopy of the hydrosilylation product compared with those of Me_2EtSiH and MAm-TBDMS, as shown in Fig. 1. In Fig. 1c, the hydrosilylation product displayed signals attributed to the dimethylethylsilyl group of Me_2EtSiH (white triangles in Fig. 1a) signals attributed to the TBDMS group of MAm-TBDMS (black triangles in Fig. 1b). Additionally, the vinyl group signals in MAm-TBDMS (white circles in Fig. 1b) were not observed while methyl group signals appeared at 0.76 ppm. These results confirm that the $B(C_6F_5)_3$-catalyzed hydrosilylation of MAm-TBDMS with Me_2EtSiH lead to quantitative formation of SKAm^{EtMe2}-TBDMS, and the reaction solution was used as the stock solution for subsequent GTP.

Synthesis of α-end hydroxyl functionalized PDEAm

In the GTP of DEAm with $[DEAm]_0/[SKAm^{Me2Et}\text{-}OTBDMS]_0$ = 50, Me_3SiNTf_2 was used as the organocatalyst. DEAm was quantitatively polymerized to afford a poly(*N*,*N*-diethylacrylamide) with an OTBDMS-protected hydroxyl group (PDEAm-OTBDMS). Fig. 2a displays the ^{1}H NMR spectrum of PDEAm$_{50}$-OTBDMS showing signals for methylene protons at 2.39–2.80 ppm (white circles) together with $-NCH_2CH_3$ group signals at 0.95–1.33 ppm (black squares). After deprotecting PDEAm$_{50}$-OTBDMS to PDEAm$_{50}$-OH using tetrabutylammonium fluoride (TBAF), a very small portion divided from the polymerization mixture was purified to isolate and characterize PDEAm$_{50}$-OH. As shown in Fig. 2b, the PDEAm$_{50}$-OH proton signals due to the TBDMS group of PDEAm$_{50}$-OTBDMS (black triangles in Fig. 2a) have completely disappeared. Table S1† lists the polymerization results. The targeted PDEAm$_{50}$-OH obtained had a SEC-measured $M_{n,SEC}$ of 6.2 kg mol^{-1} and low Đ of 1.08 that well agreed with calculated number-average molecular weights ($M_{n,calcd}$) of 6.4 kg mol^{-1}. Similarly, for GTP using $[DEAm]_0/[SKAm^{Me2Et}\text{-}OTBDMS]_0$ of 30–90, the obtained PDEAmOHs possessed the targeted SEC-measured M_n along with low Đs, as shown in Fig. 3a.

Synthesis of PDEAm-*b*-PEs

We planned the preparation of PDEAm$_x$-*b*-PEs$_y$ in which *x* and *y* denote the degree of polymerizations for the PDEAm and PEs segments (DP*x* and DP*y*, respectively). Three types of polyesters (PEs) were selected as the second segments of block copolymers, including poly(ε-caprolactone) (PCL), poly(trimethylene carbonate) (PTMC), and poly(L-lactide) (PLLA). Table 1 lists the result of the second polymerizations. For a representative example, PDEAm$_{50}$-OH was used as the macroinitiator for the ROP of ε-caprolactone (ε-CL) using *t*-Bu-P_2 as the polymerization organocatalyst. After the polymerization with a $[PDEAm_{50}\text{-}OH]_0/[\varepsilon\text{-}CL]_0$ of 50 for 24 h, ε-CL was quanti-

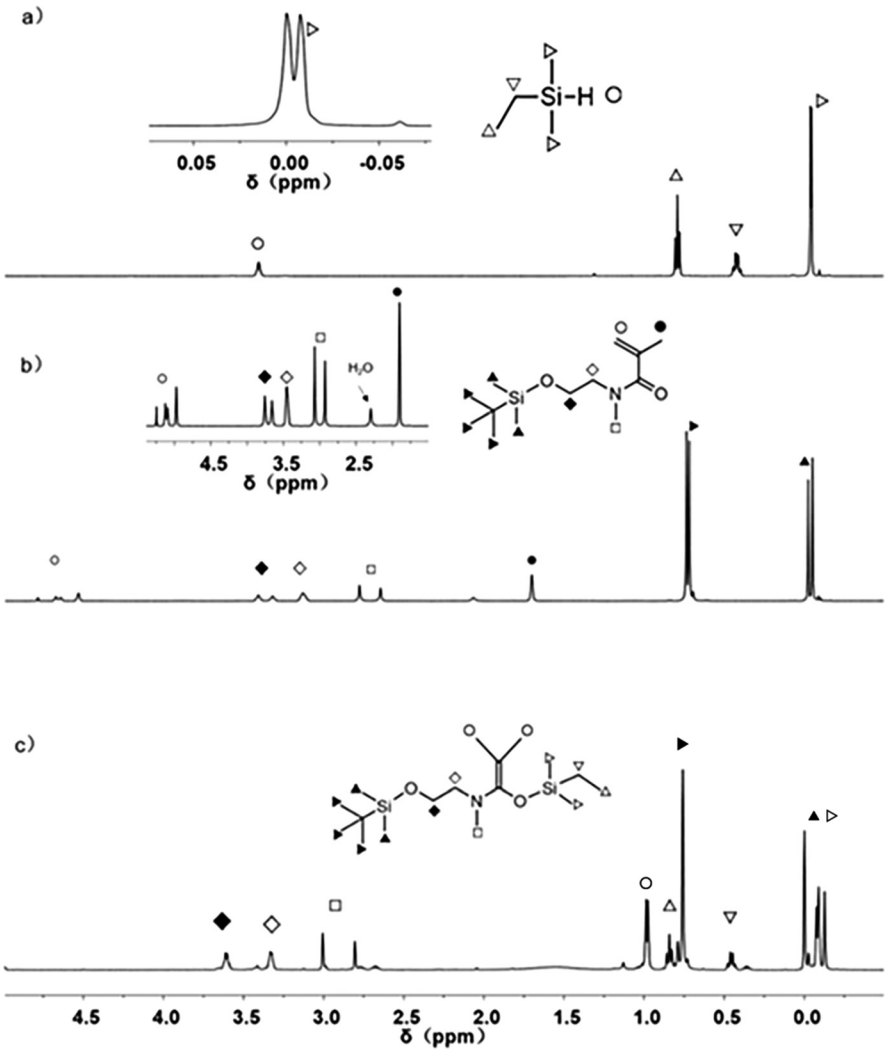

Fig. 1 ^{1}H NMR spectra of (a) Me_2EtSiH, (b) MAm-TBDMS, and (c) the hydrosilylation product measured in $CDCl_3$.

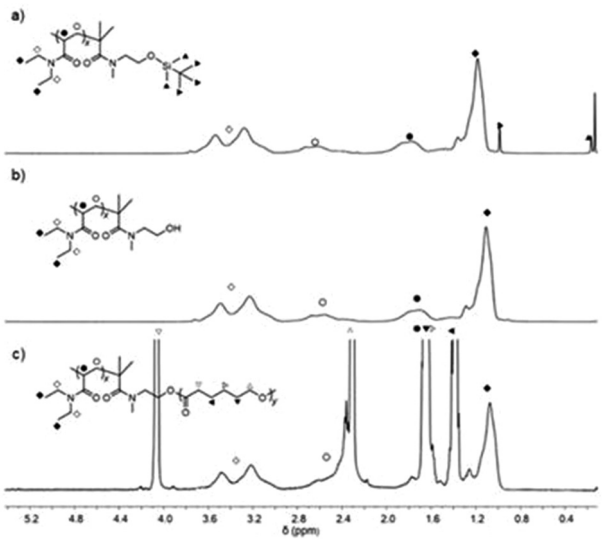

Fig. 2 ^{1}H NMR spectra of (a) PDEAm-TBDMS, (b) PDEAm-OH, and (c) PDEAm-*b*-PCL in $CDCl_3$.

tatively consumed and the resulting copolymer structure was confirmed by ^{1}H NMR. Signals corresponding to the methylene protons of the PCL segment along with the PDEAm segment were observed at 1.38, 1.65, 2.31, and 4.06 ppm (black and white triangles in Fig. 2c), indicating PDEAm$_x$-*b*-PCL$_y$ was successfully produced. The $M_{n,SEC}$ of 12.3 kg mol^{-1} agreed well with the $M_{n,calcd}$ of 12.0 kg mol^{-1} and $Đ$ was the low value of 1.10. We prepared seven samples of well-defined PDEAm$_x$-*b*-PCL$_y$ copolymers in total with diverse DP*x*/DP*y* ratios as shown in Fig. 3.

In place of ε-CL, trimethylene carbonate (TMC) or L-lactide (L-LA) were used as the second monomers to afford the corresponding block copolymers, and ^{1}H NMR spectroscopy was used to confirm the structures (Fig. S3†). In total, 14 additional samples of PDEAm-*b*-PTMC and PDEAm-*b*-PLLA, block copolymers formed from PTMC and PLLA, were prepared with targeted molecular weights (Tables S2 and S3,† respectively) and narrow *Đ*s (Fig. S1 and S2,† respectively).

In the ^{1}H NMR spectra of PDEAm-*b*-PEs, the molecular weight of PE was difficult to determine because of the overlap

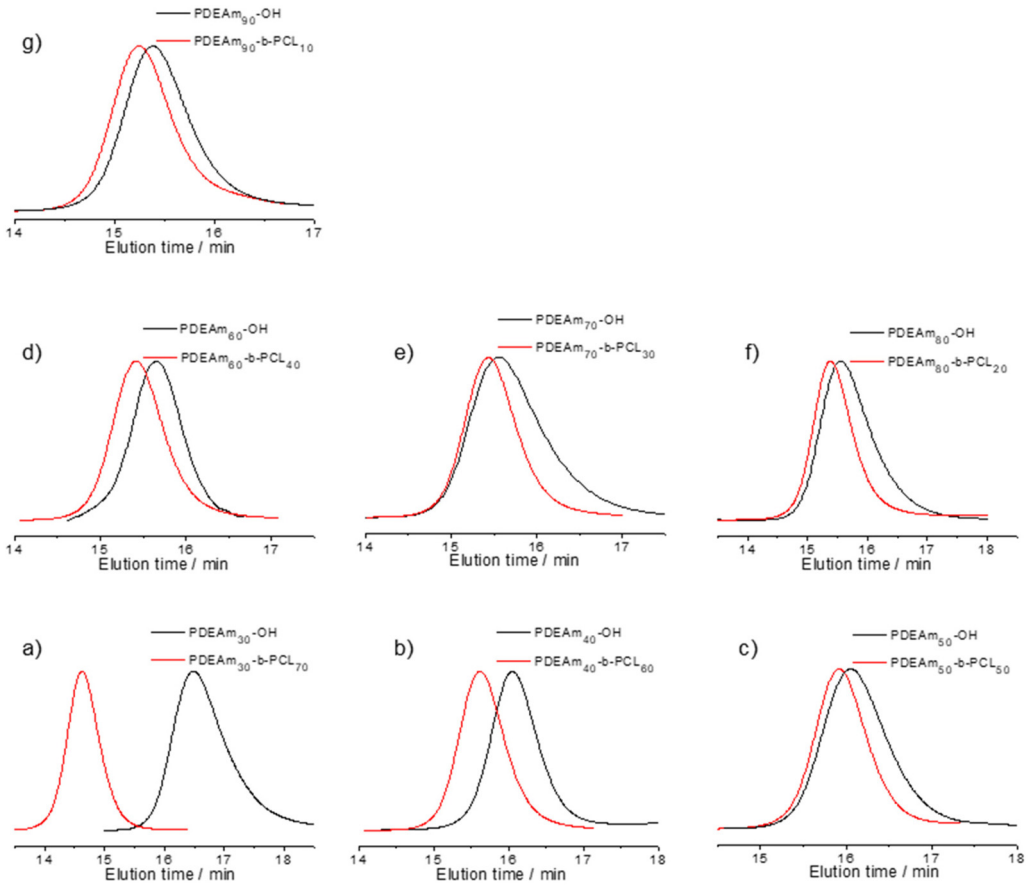

Fig. 3 SEC traces of PDEAm$_x$-OH and PDEAm$_x$-*b*-PCL$_y$ in $CDCl_3$: (a) x/y = 30/70, (b) x/y = 40/60, (c) x/y = 50/50, (d) x/y = 60/40, (e) x/y = 70/30, (f) x/y = 80/20, and (g) x/y = 90/10.

Table 1 One-pot synthesis of PDEAm-*b*-PCL by ROP of ε-CL using PDEAm-OH as the macroinitiator and *t*-Bu-P$_2$ as the organocatalyst[a]

Sample code	$[\varepsilon\text{-CL}]_0/[\text{PDEAm-OH}]_0$	$M_{n,calcd}$ [b]/kg mol^{-1}	$M_{n,SEC}$ ($Đ$)[c]/kg mol^{-1}
PDEAm$_{30}$-*b*-PCL$_{70}$	70	11.7	11.8 (1.13)
PDEAm$_{40}$-*b*-PCL$_{60}$	60	11.8	11.5 (1.11)
PDEAm$_{50}$-*b*-PCL$_{50}$	50	12.0	12.3 (1.10)
PDEAm$_{60}$-*b*-PCL$_{40}$	40	12.1	12.0 (1.12)
PDEAm$_{70}$-*b*-PCL$_{30}$	30	12.2	12.8 (1.17)
PDEAm$_{80}$-*b*-PCL$_{20}$	20	12.4	13.2 (1.07)
PDEAm$_{90}$-*b*-PCL$_{10}$	10	12.6	13.9 (1.11)

[a] PDEAm-OH, 0.20 mmol; $[\varepsilon\text{-CL}]_0$, 1.0 mol L^{-1}; solvent, CH_2Cl_2; room temperature; argon atmosphere; polymerization time, 24 h; monomer conversion determined by ^{1}H NMR in $CDCl_3$, >99%. [b] $M_{n,calcd}$ = (MW of PDEAm-OH) + $[\varepsilon\text{-CL}]_0/[\text{PDEAm-OH}]_0$ × (monomer conversion) × (MW of ε-CL) + (M.W. of H) × 2. [c] Determined by SEC calibrated against poly(methyl methacrylate) standards.

of the PDEAm and PE absorptions. However, the synthesis of PDEAm-*b*-PE was performed by the ROP of cyclic ester monomers using a PDEAm-OH with a known molecular weight, which was beforehand prepared in a one-pot polymerization system, as a macroinitiator. Moreover, all cyclic ester monomers were quantitatively consumed, and the SEC traces of the resulting PDEAm-*b*-PEs were clearly shifted toward high molecular weight region compared to PDEAm-OH, with their Đs ranging from 1.07 to 1.20 smaller. From these results, we concluded that PDEAm-*b*-PE was synthesized as designed. For the sample code of PDEAm$_x$-*b*-PCL$_y$, *x* and *y* values are used an initial molar ratio of $[\text{MAm-OTBDMS}]_0/[\text{DEAm}]_0/[\varepsilon\text{-CL, TMC, or L-LA}]_0$.

Thermoresponsive properties

We prepared a total of 21 PDEAm$_x$-*b*-PES$_y$ samples, including PDEAm$_x$-*b*-PCL$_y$, PDEAm$_x$-*b*-PTMC$_y$, and PDEAm$_x$-*b*-PLLA$_y$, with diverse DP*x*/DP*y* ratios of 90/10, 80/20, 70/30, 60/40, 50/50, 40/60, and 30/70. Unexpectedly, all of the obtained copolymers were water-soluble at room temperature, even hydrophobic PEs-enriched PDEAm$_{30}$-*b*-PES$_{70}$. On the other hand, all solutions became turbid upon heating, indicating that these PDEAm$_x$-*b*-PES$_y$ copolymers were thermoresponsive. Fig. 4 shows the plots of optical transmittance at 500 nm as a function of temperature (cloud point curves) for the aqueous solutions of PDEAm$_x$-*b*-PES$_y$ copolymers. Table 2 lists the T_{cp} values determined from Fig. 4. Fig. 5 shows the plots of T_{cp} values against the DP*x* values for the PDEAm$_x$-*b*-PES$_y$ systems together with those for the PDEAm$_x$-OH starting homopolymer

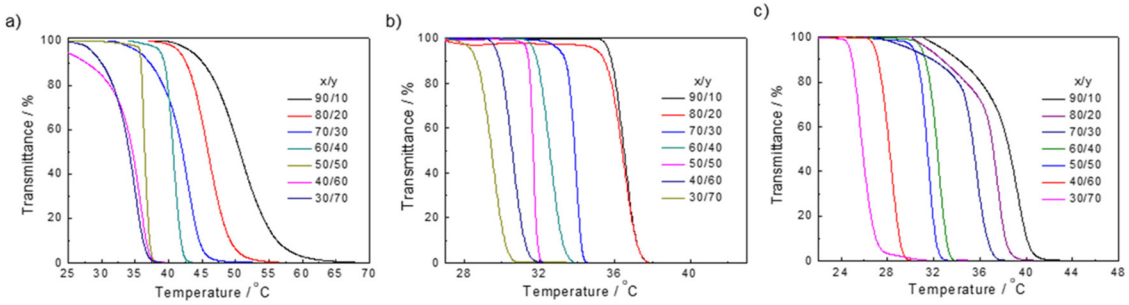

Fig. 4 UV-vis absorption spectra in water (3 g L^{-1}) at different temperatures of PDEAm-*b*-PEs: (a) PDEAm$_x$-*b*-PCL$_y$, (b) PDEAm$_x$-*b*-PTMC$_y$, and (c) PDEAm$_x$-*b*-PLLA$_y$.

Table 2 T_{cp} and R_h of PDEAm-*b*-PEs

Sample code	T_{cp} [a]	R_h [b]/nm	
		25 °C	55 °C
PDEAm$_{30}$-*b*-PCL$_{70}$	35.5	112.0	436.8
PDEAm$_{40}$-*b*-PCL$_{60}$	36.0	114.2	434.0
PDEAm$_{50}$-*b*-PCL$_{50}$	39.0	110.4	400.8
PDEAm$_{60}$-*b*-PCL$_{40}$	42.2	110.2	337.6
PDEAm$_{70}$-*b*-PCL$_{30}$	44.1	102.3	322.1
PDEAm$_{80}$-*b*-PCL$_{20}$	47.5	99.7	314.5
PDEAm$_{90}$-*b*-PCL$_{10}$	50.8	98.0	266.2
PDEAm$_{30}$-*b*-PTMC$_{70}$	29.7	238.5	720.5
PDEAm$_{40}$-*b*-PTMC$_{60}$	30.5	227.7	675.3
PDEAm$_{50}$-*b*-PTMC$_{50}$	31.0	221.0	629.7
PDEAm$_{60}$-*b*-PTMC$_{40}$	32.9	197.0	607.5
PDEAm$_{70}$-*b*-PTMC$_{30}$	34.7	171.4	531.8
PDEAm$_{80}$-*b*-PTMC$_{20}$	35.9	168.4	515.4
PDEAm$_{90}$-*b*-PTMC$_{10}$	36.1	163.9	480.0
PDEAm$_{30}$-*b*-PLLA$_{70}$	25.2	494.6	1431.0
PDEAm$_{40}$-*b*-PLLA$_{60}$	27.3	480.0	1259.0
PDEAm$_{50}$-*b*-PLLA$_{50}$	31.5	478.8	823.1
PDEAm$_{60}$-*b*-PLLA$_{40}$	32.4	454.9	745.5
PDEAm$_{70}$-*b*-PLLA$_{30}$	35.2	421.9	686.6
PDEAm$_{80}$-*b*-PLLA$_{20}$	37.1	412.5	678.1
PDEAm$_{90}$-*b*-PLLA$_{10}$	38.1	386.0	524.6

[a] Determined by UV–vis measurements in water (3 g L^{-1}). [b] Determined by dynamic light scattering (DLS) measurements in water (3 g L^{-1}).

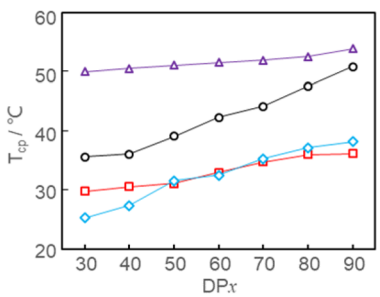

Fig. 5 Dependence of T_{cp} on DPx for PDEAm$_x$-OH (Δ), PDEAm$_x$-*b*-PCL$_y$ (○), PDEAm$_x$-*b*PTMC$_y$ (□), and PDEAm$_x$-*b*-PLLA$_y$ (◊).

system (T_{cp}s are listed in Table S1†). A trend can be observed for T_{cp}s: PDEAm$_x$-OH > PDEAm$_x$-*b*-PCL$_y$ > PDEAm$_x$-*b*-PTMC$_y$ ≈ PDEAm$_x$-*b*-PLLA$_y$. This result could be expected because the introduced PEs units were hydrophobic, which decrease the T_{cp} values compared to that for starring PDEAm$_x$-OH.[51–54] The dependence of T_{cp} on the DPx was very small for the PDEAm$_x$-OH system and only ranged from 49.9 °C to 53.8 °C. Contrastingly, the dependence was noticeable in the PDEAm$_x$-*b*-PCL$_y$ system where T_{cp} increased from 35.5 °C to 5 °C with increasing DPx content from 30% to 90%. This trend was also observed for the other PDEAm$_x$-*b*-PEs$_y$ systems where the T_{cp}s increased from 29.7 °C to 36.1 °C and from 25.2 °C to 38.1 °C for the PDEAm$_x$-*b*-PTMC$_y$ and PDEAm$_x$-*b*PLLA$_y$ systems, respectively. Addition thermoresponsive trends were revealed upon closer examination of PDEAm$_x$-*b*-PEs$_y$ within their respective PEs series.

The ^{1}H NMR spectra for a series of PDEAm$_x$-*b*-PEs$_y$ copolymers in D_2O were measured at different temperatures to characterize their phase transition behaviors.[55,56] Fig. 6 displays the ^{1}H NMR spectra for PDEAm$_{30}$-*b*-PCL$_{70}$ (T_{cp} = 35.5 °C) at 30, 35, and 40 °C in D_2O. Focusing on the signals attributed to the PCL (black and white triangles) and PDEAm segments (black and white squares), at 30 °C, we expected that signals due to the PDEAm segments would appear, while those for the PCL segments would not be observed because molecular motion of the protons in the hydrophobic PCL segments should be significantly suppressed by their hydrophobic interactions. However, we obtained clear signals for both PDEAm and PCL segments. A possible interpretation of this result is that the hydrophobic interactions among the PCL segments were not very strong. This hypothesis may be supported in the forthcoming discussion. For the measurements at 35 °C and 40 °C, nearly all the PCL and PDEAm peaks disappeared. At temperatures higher than T_{cp}, PDEAm$_x$-*b*-PCL$_y$ aggregates to precipitate out, resulting in loss of sample signals since the copolymer has left the solution phase. Similar results were obtained for the PDEAm$_x$-*b*-PTMC$_y$ and PDEAm$_x$-*b*-PLLA$_y$ systems (Fig. S4†).

To provide reliable insights into the phase transition behavior, we performed dynamic light scattering (DLS) measurements at 25 °C (Fig. S5, S7, and S9†) and 55 °C (Fig. S6, S8, and S10†). The DLS measurements confirmed that all of PDEAm-*b*-PEs copolymers exist as particles in aqueous solutions at both 25 °C and 55 °C, while their average R_h values varied significantly depending on the measurement tempera-

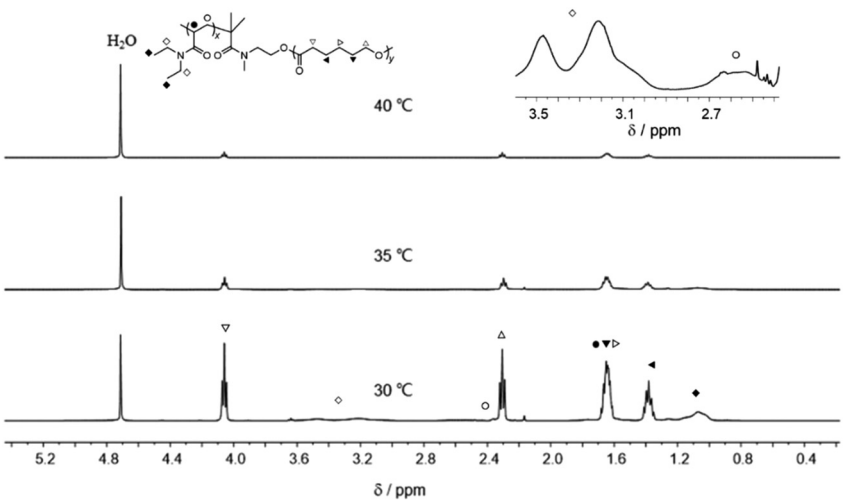

Fig. 6 ^{1}H NMR spectra of PDEAm$_{30}$-*b*-PCL$_{70}$ measured at 30, 35, and 40 °C in D_2O.

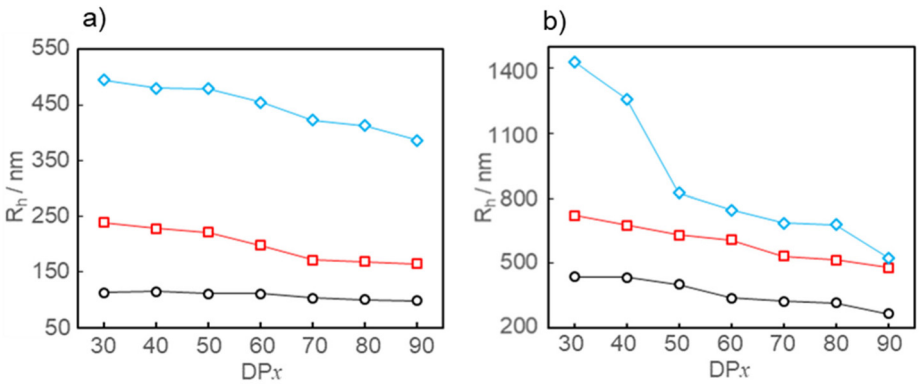

Fig. 7 Dependence of R_h on DP$_x$ for PDEAm$_x$-*b*-PCL$_y$ (○), PDEAm$_x$-*b*-PTMC$_y$ (□), and PDEAm$_x$-*b*-PLLA$_y$ (◊) measured in water at: (a) 25 °C and (b) 55 °C.

ture and the resulting thermoresponsive structures (Table 2). Fig. 7a and b display plots of the observed R_h on DP$_x$ for a series of PDEAm$_x$-*b*-PEs$_y$'s measured at 25 °C and 55 °C, respectively. A general result is that the R_h values at 25 °C (98.0–494.6 nm) are significantly smaller compared to those at 55 °C (266.2–1431.0 nm). Another observed trend was that the R_h values increased in the order of PDEAm$_x$-*b*-PCL$_y$ < PDEAm$_x$-*b*-PTMC$_y$ ≪ PDEAm$_x$-*b*-PLLA$_y$.

Examining each sample individually, the measurements at 25 °C (below T_{cp}) indicate that PDEAm$_x$-*b*-PCL$_y$ exists as particles with a R_h of 98.0–114.2 nm (Fig. S5†). Notably, the particle size was somewhat larger if the morphology of the aggregate was a distinct core–shell micelle structure, indicating that PDEAm$_x$-*b*-PCL$_y$ existed as an aggregate with a randomly mixed micelle structure morphology below its T_{cp}. This hypothesis would be consistent with the discussion from the NMR section where the molecular motions for the hydrophobic PCL segments were not significantly restricted. The R_h at 25 °C increased with increasing DP*x* in PDEAm$_x$-*b*-PCL$_y$. The measurements at 55 °C (above T_{cp}) indicated that each R_h significantly increased in the range of 266.2 nm to 436.8 nm (Fig. S6†). Notably, the distributions in the particle sizes appear broader. These results support that PDEAm$_x$-*b*-PCL$_y$ exists as a large hydrophobic cluster-like structure composed of thermoresponsive PDEAm segments and hydrophobic PCL ones above T_{cp}.

Similar results were obtained for the PDEAm$_x$-*b*-PTMC$_y$ system: the R_h values ranged from 136.9 nm to 238.5 nm at 25 °C and increased to range from 480.0 nm to 720.5 nm at 55 °C. For the PDEAm$_x$-*b*-PLLA$_y$ system, the observed particle size increases were the most significant. The R_h values ranged from 386 nm to 494.6 nm at 25 °C and increased significantly to range from 524.6 nm to 1259.0 nm at 55 °C. We would like to emphasize this featured result: that the R_h in the PDEAm$_x$-*b*-PLLA$_y$ system was considerably larger than those of PDEAm$_x$-*b*PCL$_y$ and PDEAm$_x$-*b*-PTMC$_y$ at 25 °C. Therefore, PDEAm$_x$-*b*-PLLA$_y$ formed larger and looser aggregates within these three kinds of PDEAm$_x$-*b*-PEs$_y$ copolymers.

Conclusion

A series of PDEAm$_x$-*b*-PEs$_y$ (PDEAm$_x$-*b*-PCL$_y$, PDEAm$_x$-*b*-PTMC$_y$, and PDEAm$_x$-*b*PLLA$_y$) were synthesized using the one-pot catalyst-switching method where organocatalytic GTP and ROP can be performed sequentially in the same reaction vessel by simply changing the organocatalyst. This synthetic method encourages the broadening of thermoresponsive polymer architecture libraries composed from vinyl polymers and aliphatic biodegradable polymers. In total, 21 PDEAm$_x$-*b*-PEs$_y$ samples with different DP$_x$/DP$_y$ ratios were carefully characterized in water, providing insights into their T_{cp} values. A small but crucial conclusion from characterization studies performed below T_{cp} was that PDEAm$_x$-*b*-PEs$_y$ copolymers seem to exist as randomly mixed loose micellar aggregates and not distinct core–shell micelle structures. Notably, PDEAm$_x$-*b*-PLLA$_y$ formed larger and looser aggregates within the three types of PDEAm$_x$-*b*-PEs$_y$ copolymers studied, thus leading to lower T_{cp} temperatures.

Conflicts of interest

There are no conflicts to declare.

References

1 Y. Zhao, T. Bai, Q. Shao, S. Jiang and A. Q. Shen, *Polym. Chem.*, 2015, **6**, 1066–1077.
2 D. Wang, H. Ren, X. Wang and X. Wang, *Macromolecules*, 2008, **41**, 9382–9388.
3 S. J. T. Rezaei, M. R. Nabid, H. Niknejad and A. A. Entezami, *Int. J. Pharm.*, 2012, **437**, 70–79.
4 J. Mao, X. Ji and S. Bo, *Macromol. Chem. Phys.*, 2011, **212**, 744–752.
5 N. Toshikj, J. J. Robin and S. Blanquer, *Eur. Polym. J.*, 2020, **127**, 109599.
6 J. Sun, S. Fransen, X. Yu and D. Kuckling, *Polym. Chem.*, 2018, **9**, 3287–3296.
7 Y. Shao, Y. G. Jia, C. Shi, J. Luo and X. X. zhu, *Biomacromolecules*, 2014, **15**, 1837–1844.
8 H. Y. Lee, S. H. Park, J. H. Kim and M. S. Kim, *Polym. Chem.*, 2017, **8**, 6606–6616.
9 R. Tang, W. Ji and C. Wang, *Macromol. Biosci.*, 2010, **10**, 192–201.
10 A. L. Brocas, M. Gervais, S. Carlotti and S. Pispas, *Polym. Chem.*, 2012, **3**, 2148.
11 L. Yao, L. Yu, L. Li and J. Kou, *J. Phys.: Conf. Ser.*, 2020, **1575**, 012161.
12 G. Barouti, K. Jarnouen, S. Cammas-Marion, P. Loyer and S. M. Guillaume, *Polym. Chem.*, 2015, **6**, 5414–5429.
13 S. Imai, Y. Hirai, C. Nagao, M. Sawamoto and T. Terashima, *Macromolecules*, 2018, **51**, 398–409.
14 D. Zehm, A. Laschewsky, H. Liang and J. P. Rabe, *Macromolecules*, 2011, **44**, 9635–9641.
15 W. H. Binder, D. Gloger, H. Weinstabl, G. Allmaier and E. Pittenauer, *Macromolecules*, 2007, **40**, 3097–3107.
16 G. Lu, X. Jiang, Y. Li, X. Lv and X. Huang, *RSC Adv.*, 2015, **5**, 74947–74952.
17 C. Lv, Z. Zhang, J. Gao, J. Xue, J. Li, J. Nie, J. Xu and B. Du, *Macromolecules*, 2018, **51**, 1013610149.
18 K. Y. Cho, J. W. Choi, S. H. Lee, S. S. Hwang and K. Y. Baek, *Polym. Chem.*, 2013, **4**, 2400.
19 J. Škvarla, J. Zedník, M. Šlouf, S. Pispas and M. Štěpánek, *Eur. Polym. J.*, 2014, **61**, 124–132.
20 R. Freitag, T. Baltes and M. Eggert, *J. Polym. Sci., Part A: Polym. Chem.*, 1994, **32**, 3019–3030.
21 M. Kobayashi, S. Okuyama, T. Ishizone and S. Nakahama, *Macromolecules*, 1999, **32**, 6466–6477.
22 A. Narumi, S. I. Sato, X. Shen and T. Kakuchi, *Polym. Chem.*, 2022, **13**, 1293–1319.
23 S. Kikuchi, Y. Chen, E. Ichinohe, K. Kitano, S. Sato, Q. Duan, X. Shen and T. Kakuchi, *Macromolecules*, 2016, **49**, 4828–4838.
24 J. Li, S. Kikuchi, S. Sato, Y. Chen, L. Xu, B. Song, Q. Duan, Y. Wang, T. Kakuchi and X. Shen, *Macromolecules*, 2019, **52**, 7207–7217.
25 S. Kikuchi, Y. Chen, K. Kitano, K. Takada, T. Satoh and T. Kakuchi, *Polym. Chem.*, 2015, **6**, 6845–6856.
26 S. Kikuchi, Y. Chen, K. Kitano, S. Sato, T. Satoh and T. Kakuchi, *Macromolecules*, 2016, **49**, 3049–3060.
27 F. Nederberg, E. F. Connor, M. Möller, T. Glauser and J. L. Hedrick, *Angew. Chem., Int. Ed.*, 2001, **40**, 2712–2715.
28 T. He, Y. Wang, A. Narumi, L. Xu, S. I. Sato, X. Shen and T. Kakuchi, *Polymers*, 2021, **13**, 3873.
29 K. Makiguchi, T. Satoh and T. Kakuchi, *J. Polym. Sci., Part A: Polym. Chem.*, 2011, **49**, 3769–3777.
30 T. Kitayama, H. Yamaguchi, T. Kanzawa and T. Hirano, *Polym. Bull.*, 2000, **45**, 97–104.
31 T. Horváth, K. Marossy and T. J. Szabó, *J. Therm. Anal. Calorim.*, 2021, **147**, 2221–2227.
32 X. Wang, S. Cui, Z. Li, S. Kan, Q. Zhang, C. Zhao, H. Wu, J. Liu, W. Wu and K. Guo, *Polym. Chem.*, 2014, **5**, 6051–6059.
33 C. Thomas and B. Bibal, *Green Chem.*, 2014, **16**, 1687–1699.
34 S. Liu, C. Ren, N. Zhao, Y. Shen and Z. Li, *Macromol. Rapid Commun.*, 2018, **39**, 1800485.
35 I. Jain and P. Malik, *Eur. Polym. J.*, 2021, **150**, 110412.
36 S. Tempelaar, L. Mespouille, O. Coulembier, P. Dubois and A. P. Dove, *Chem. Soc. Rev.*, 2013, **42**, 1312–1336.
37 K. Makiguchi, T. Satoh and T. Kakuchi, *Macromolecules*, 2011, **44**, 1999–2005.
38 K. Makiguchi, Y. Ogasawara, S. Kikuchi, T. Satoh and T. Kakuchi, *Macromolecules*, 2013, **46**, 1772–1782.
39 K. Makiguchi, S. Kikuchi, K. Yanai, Y. Ogasawara, S. Sato, T. Satoh and T. Kakuchi, *J. Polym. Sci., Part A: Polym. Chem.*, 2014, **52**, 1047–1054.
40 R. A. Alshumrani and N. Hadjichristidis, *Polym. Chem.*, 2017, **8**, 5427–5432.
41 J. K. Palacios, J. Zhao, N. Hadjichristidis and A. J. Müller, *Macromolecules*, 2017, **50**, 9683–9695.

42 H. Alamri, J. Zhao, D. Pahovnik and N. Hadjichristidis, *Polym. Chem.*, 2014, **5**, 5471–5478.
43 J. Zhao, D. Pahovnik, Y. Gnanou and N. Hadjichristidis, *Polym. Chem.*, 2014, **5**, 3750–3753.
44 J. Zhao, D. Pahovnik, Y. Gnanou and N. Hadjichristidis, *Macromolecules*, 2014, **47**, 3814–3822.
45 V. Ladelta, J. D. Kim, P. Bilalis, Y. Gnanou and N. Hadjichristidis, *Macromolecules*, 2018, **51**, 2428–2436.
46 H. Alamri and N. Hadjichristidis, *Polym. Chem.*, 2016, **7**, 3225–3228.
47 J. Zhao and N. Hadjichristidis, *Polym. Chem.*, 2015, **6**, 2659–2668.
48 J. Zhao, D. Pahovnik, Y. Gnanou and N. Hadjichristidis, *J. Polym. Sci., Part A: Polym. Chem.*, 2014, **53**, 304–312.
49 M. S. Zaky, G. Guichard and D. Taton, *Macromol. Rapid Commun.*, 2022, **43**, 2200395.
50 M. Liu, B. Wang, L. Pan, X. H. Liu and Y. S. Li, *Polym. Chem.*, 2022, **13**, 3451.
51 S. S. Patil and P. P. Wadgaonkar, *J. Polym. Sci., Part A: Polym. Chem.*, 2017, **55**, 1383–1396.
52 B. Lu, L. Li, L. Wei, X. Guo, J. Hou and Z. Liu, *RSC Adv.*, 2016, **6**, 50993–51004.
53 H. Ajiro, Y. Takahashi and M. Akashi, *Macromolecules*, 2012, **45**, 2668–2674.
54 Y. S. Jo, D. K. Kim and M. Muhammed, *J. Mater. Sci.: Mater. Med.*, 2004, **15**, 1291–1295.
55 T. He, Y. Wang, A. Narumi, L. Xu, S. I. Sato, X. Shen and T. Kakuchi, *Polym. Chem.*, 2021, **12**(17), 2580–2591.
56 J. Li, S. Mizutani, S. I. Sato, A. Narumi, O. Haba, S. Kawaguchi, M. Kikuchi, T. Kakuchi and X. Shen, *Polym. Chem.*, 2020, **11**(13), 2346–2359.